Arch. Metall. Mater., Vol. 61 (2016), No 3, p. 1363–1370

DOI: 10.1515/amm-2016-0224

A. CZUPRYŃSKI*,#, J. GÓRKA*, M. ADAMIAK**, B. TOMICZEK**

TESTING OF FLAME SPRAYED Al_2O_3 MATRIX COATINGS CONTAINING TiO_2

The paper presents the results of the properties of flame sprayed ceramic coatings using oxide ceramic materials coating of a powdered aluminium oxide (Al_2O_3) matrix with 3% titanium oxide (TiO_2) applied to unalloyed S235JR grade structural steel. A primer consisting of a metallic Ni-Al-Mo based powder has been applied to plates with dimensions of 5×200×300 mm and front surfaces of Ø40×50 mm cylinders. Flame spraying of primer coating was made using a RotoTec 80 torch, and an external coating was made with a CastoDyn DS 8000 torch. Evaluation of the coating properties was conducted using metallographic testing, phase composition research, measurement of microhardness, substrate coating adhesion (acc. to EN 582:1996 standard), erosion wear resistance (acc. to ASTM G76-95 standard), and abrasive wear resistance (acc. to ASTM G65 standard) and thermal impact. The testing performed has demonstrated that flame spraying with 97% Al_2O_3 powder containing 3% TiO_2 performed in a range of parameters allows for obtaining high-quality ceramic coatings with thickness up to ca. 500 μm on a steel base. Spray coating possesses a structure consisting mainly of aluminium oxide and a small amount of $NiAl_{10}O_{16}$ and $NiAl_{32}O_{49}$ phases. The bonding primer coat sprayed with the Ni-Al-Mo powder to the steel substrate and external coating sprayed with the 97%Al_2O_3 powder with 3% TiO_2 addition demonstrates mechanical bonding characteristics. The coating is characterized by a high adhesion to the base amounting to 6.5 MPa. Average hardness of the external coating is ca. 780 HV. The obtained coatings are characterized by high erosion and abrasive wear resistance and the resistance to effects of cyclic thermal shock.

Keywords: Flame spray process, Coating, Ceramic powder, Abrasive wear resistance, Erosion wear resistance, Adhesion strength

1. Introduction

Thermal spraying methods have been notably developed within the last years, due to more and more technologically advanced heat sources and until now new unused coating materials [1-3]. Currently, about 70% of the industrial use of this technology consists of manufacturing new machinery parts and equipment demanding a high quality of execution and suitable surface properties. The rapid development of thermal spraying technologies is also the result of an increase of operating parameters of machines and equipment related to high loads and velocities causing their accelerated wear and the necessity of efficient regeneration.

The use of thermally sprayed coatings not only results in an increased level of durability of steel structures against a corrosive environment, but also contributes to a lengthened life cycle of textile machine parts, casting moulds, rollers in steel plant transporters, pumps and mixers elements, injection moulding machines, and improved durability and reliability of power plant boilers [4-6]. Because of their high resistance to corrosion, erosion and abrasion as well as their hardness and creep resistance an increasing amount of sprayed coatings are composed of engineering ceramic materials, especially when forming excellent thermal and electrical barriers is required. Particularly noteworthy are ceramic materials based on aluminium oxide Al_2O_3. The aim of the study was to produce a ceramic coating on the base of Al_2O_3 with a low content of TiO_2 by cold flame spraying (with minimal pre heating to the range of 40°C) to ensure high hardness and high adhesion. Formation of thin ceramic coatings by flame spraying with such characteristics is relatively difficult to obtain [7-11]. Parameter optimization of spraying and the use of the primer coating such as: Ni-Al-Mo, could minimize the stress level between the substrate material and the coating, at the same time ensuring its high resistance to abrasive wear, erosive wear and also to the cyclic heat stroke. Thermal and electrical barrier flame sprayed coating containing Al_2O_3 are used in many cases, i.e. electronic elements, isolation components of ignition plugs, power turbines, high temperature resistant and thermally affected portions of combustion chambers in a modern car and aircraft engines [12-18].

2. Experimental procedure and results

The aim of this study was to develop the technical conditions of flame powder spraying and to determine operating characteristics of the coating composed of ceramic powder Al_2O_3 oxide on structural non-alloyed steel S235JR acc. to EN 10025-2:2004. For flame spraying, the powder was

* SILESIAN UNIVERSITY OF TECHNOLOGY, FACULTY OF MECHANICAL ENGINEERING, THE CHAIR OF WELDING, 18A KONARSKIEGO STR., 44-100 GLIWICE, POLAND

** SILESIAN UNIVERSITY OF TECHNOLOGY, FACULTY OF MECHANICAL ENGINEERING, INSTITUTE OF ENGINEERING MATERIALS AND BIOMATERIALS, 18A KONARSKIEGO STR., 44-100 GLIWICE, POLAND,

Corresponding author: artur.czuprynski@polsl.pl

comprised of 97wt%Al_2O_3 and 3wt%TiO_2. Joining powder composed of Ni-Al-Mo alloy was used as a primer coating. According to the manufacturer the 97%Al_2O_3+3%TiO_2 powder can be used for spraying without preheating (referred to as „cold type") parts such as sleeves of pumps, O-ring gaskets, sliding surfaces, pump vanes, pump rotors and electric insulators. The coating for this test is made with the chosen powder according to the manufacturer is an excellent thermal insulator and is highly resistant to thermal shock. The hardness of the coating sprayed with this powder is ca. 700 HV10. The metallic Ni-Al-Mo based powder is often used as a primer coating in order to increase their adhesion to the substrate. Flame spraying operations were conducted on 5×200×300 mm plates with head surfaces rollers of Ø40×50mm, Figure 1.

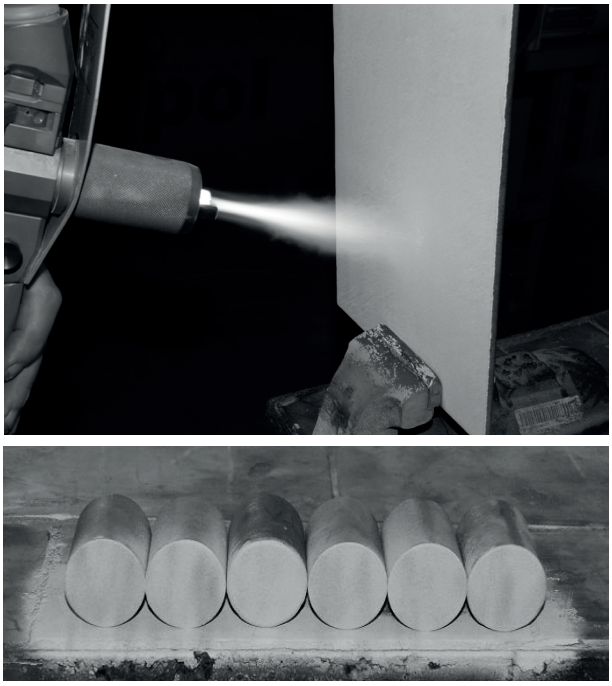

Fig. 1. View of the flame sprayed operations and samples with 97%Al_2O_3+3%TiO_2 powder

Immediately before spraying, surfaces of plates and cylinders were cleaned by grit blasting according to the requirements of the EN 13507:2010 standard. Cleaning of surfaces was done with the acute-angled grit from hardened cast iron. The spraying process consisted of the following operations:

- spraying the primer coating with a thickness from 50 to 100 μm with Ni-Al-Mo powder using RotoTec 80 torch, Table 1,
- spraying the external specific coating with ca. 500 μm thickness with 97%Al_2O_3+3%TiO_2 powder using CastoDyn DS 8000 torch, Table 2.

TABLE 1
Primer coating spraying parameters with Ni-Al-Mo powder

Type of torch:	RotoTec 80
Acetylene pressure:	0.7 [bar]
Oxygen pressure:	4.0 [bar]
Distance from torch to sprayed surface:	200 [mm]
Preheating temperature:	40 [°C]
Each time the change of torch leading angle with regard to the next coating:	900

TABLE 2
External coating spraying parameters with 97%Al_2O_3+3%TiO_2 powder

Type of torch:	CastoDyn DS 8000
Torch nozzle:	SSM 30
Powder flow for powder 97%Al_2O_3+3%TiO_2:	2 (adjustment acc. to instruction)
Acetylene pressure:	0.7 [bar]
Oxygen pressure:	4.0 [bar]
Auxiliary gas pressure (compressed air)	3.0 [bar]
Note: A primer coating made with Ni-Al-Mo powder is required	

After the spraying process, the plate covered with ceramic coating was cut into samples ready for further testing. Adhesion testing of the coating was conducted on cylinder samples.

Metallographic macroscopy of the sprayed coating surface was done using the stereoscopic microscope applying magnification from 4× to 25×.

Metallographic microscopy was conducted on metallographic specimens perpendicular to the coating, cut out of plates after flame spraying. The structure of examined coating is shown on specimens etched in a 4% solution of nitric acid (HNO_3) and ethyl alcohol (C_2H_5OH). Microscopy was conducted with magnification ranging from 100× to 1000×. The grain structure present on the plates was determined by comparison. Coating thickness was determined with a metallographic method according to the ISO 1463 1997 standard. The result was a mean value of ten measurements. Results of metallographic microscope tests allowed for the evaluation of the base material structure, the primer coating, the outer coating and its thickness after the flame spraying operation. Results of the test are shown in Figure 2 and Figure 3.

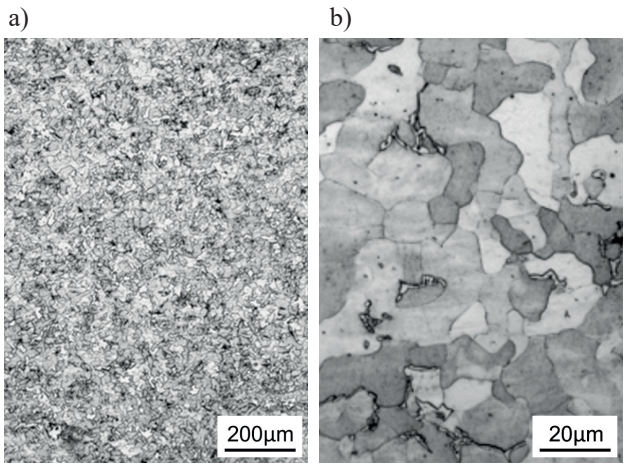

Fig.2. Fine-grained structure of ferrite with small areas of perlite in steel exposed to the flame spraying process: a) 100× mag., b) 1000× mag

Coating hardness was measured using the Vickers method. Tests were conducted in compliance with ISO 6507-1:2007 standard. Load during measurements was recorded to have between 0.1 and 5 N. Fifteen hardness measurements

were performed on cross-sectional samples, wherein six measurements were done on the outer coating (A), three on the primer coat (B) and six on the base material (C), in micro-areas marked on Figure 4. Results are shown in Table 3.

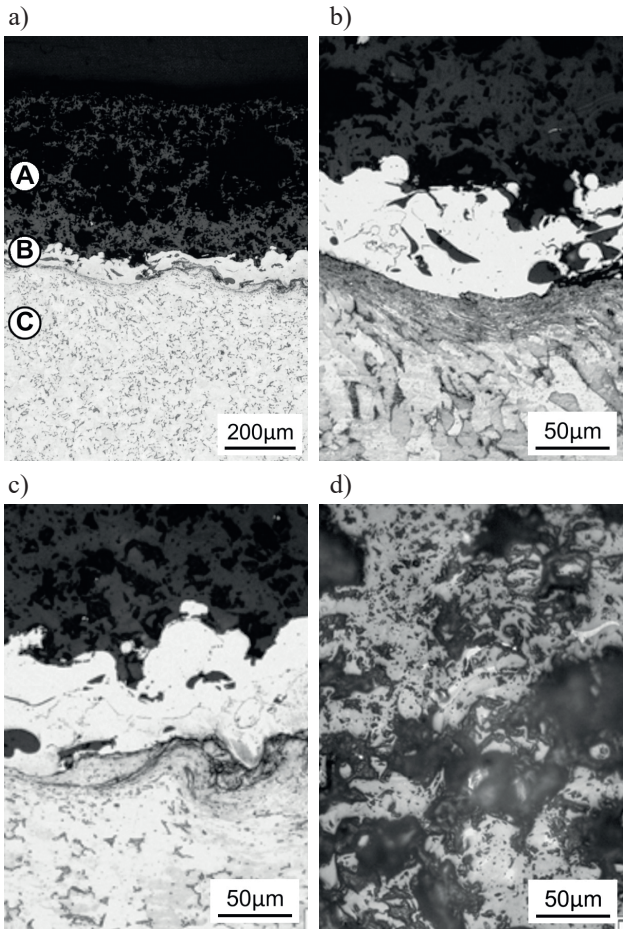

Fig. 3. View after flame spraying with 97%Al_2O_3+3%TiO_2 powder: a) outer coating structure (A), Ni-Al-Mo primer coat (B) and substrate (C), 100× mag.; b) outer coating and an image of the outer coating seam boundary, 400× mag.; c) structure of the primer coat over the area of deformed steel with developed surface line, 400× mag.; d) structure of outer coating, 400× mag.

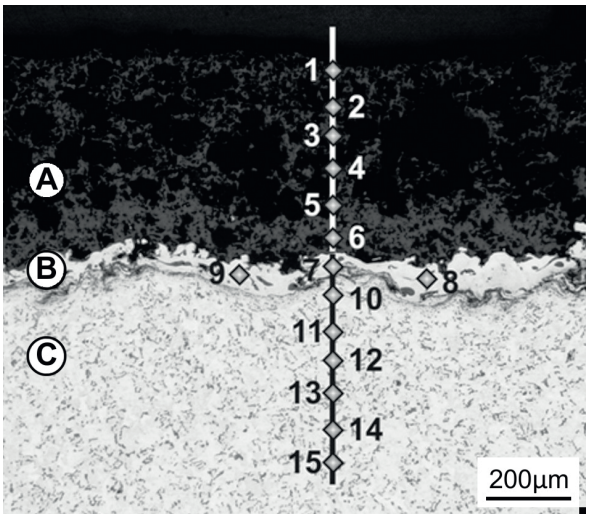

Fig. 4. Chart of hardness measurements on a transversal section of the sample after flame spraying: A – outer coating, B – primer coating, C – base material

TABLE 3
Results of hardness measurements on cross-section of sample after spraying with 97%Al_2O_3+3%TiO_2 powder

Test area	Test spot	Load [N]	HV hardness
External coating A (97%Al_2O_3+3%TiO_2)	1	5.0	747
	2	5.0	823
	3	5.0	910
	4	5.0	672
	5	5.0	762
	6	5.0	747
Primer coating B (Ni-Al-Mo)	7	0.1	469
	8	0.1	353
	9	0.1	458
Base material C (S235JR)	10	0.5	226
	11	0.5	189
	12	0.5	145
	13	0.5	131
	14	0.5	128
	15	0.5	110

X-ray examination of the sample surface after flame spraying was conducted on an x-ray diffractometer (XRD) which allowed to find the phase composition of the outer coating made with powder on alumina matrix on the primer coating composed of Ni-Al-Mo powder and substrate material composed of S235JR low-carbon steel. Results of the XRD analysis are shown on the diffractogram, Figure 5.

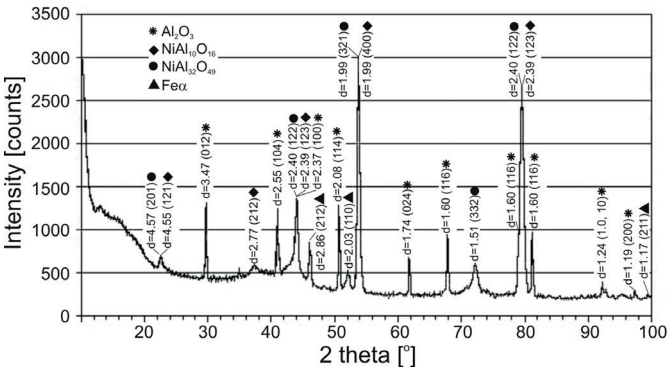

Fig. 5. Diffractogram of flame sprayed coating with 97%Al_2O_3+3%TiO_2 powder

Careful testing of the coating was performed using scanning electron microscopy (SEM). Metallographic specimens were observed under magnification from 250× to 5000×. SEM evaluation allowed determining the influence of powder type on the process and its effects on the structure of the outer coating and the concentration of micro-elements in selected areas. Observation results of the microstructures in the outer coating and primer coating are shown in Figure 6, and the results of microanalysis chemical composition in Figure 7 and Figure 8.

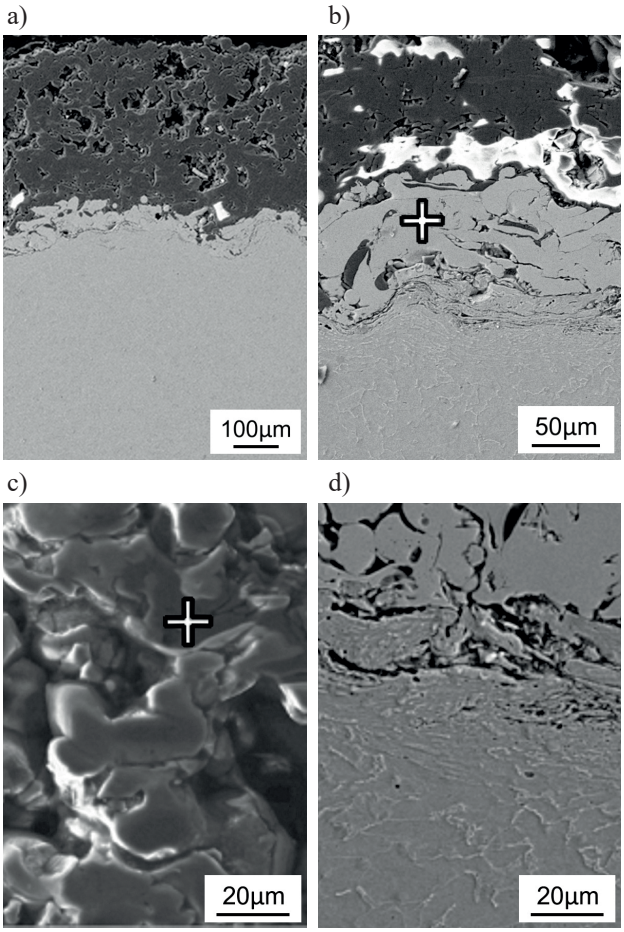

Fig. 6. View of the coating after flame spraying with 97%Al_2O_3+3%TiO_2 powder: a) structure of the external coating with primer coating and base material with visible empty spaces in diverse sizes in the external coating of sample; b) small amount of empty spaces in the external coating in border area to primer coating; c) the external coating structure; d) area of base material and primer coating

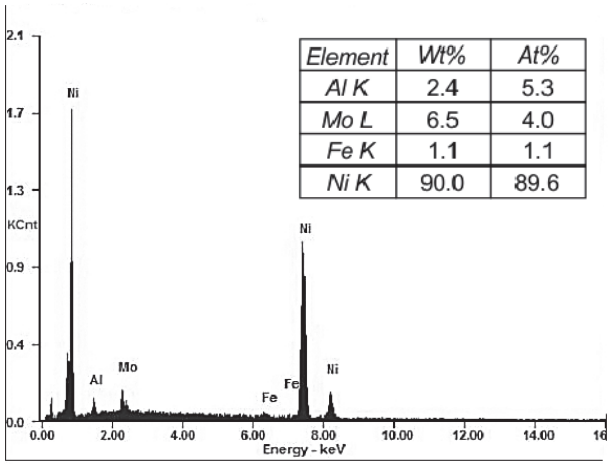

Figure 7. Microanalysis of chemical composition of area from Figure 6 b)

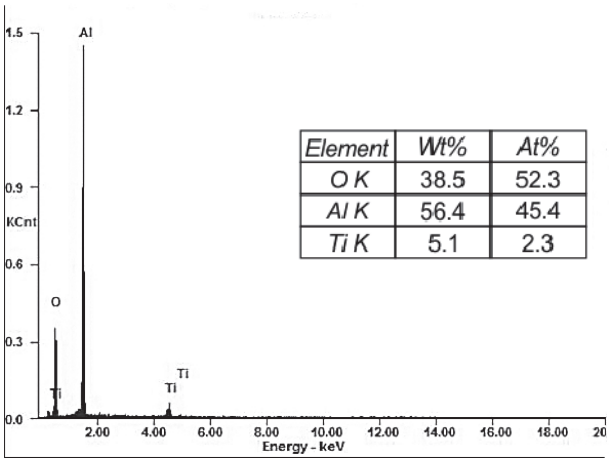

Figure 8. Microanalysis of chemical composition of area from Figure 6 c)

Examination of the coating surface roughness was evaluated using profilometry in accordance with ISO 4287:1999/A1:2010 standard. Roughness was examined on the sample surface with dimensions 5×200×300 mm immediately after the flame spraying process was completed. Measurement was carried out on five sections of length l=25 mm in two perpendicular directions. The roughness of sprayed surfaces was determined following basic parameters namely; R_a – mean roughness, R_z – surface roughness depth and R_{max} – maximum roughness depth, Figure 9.

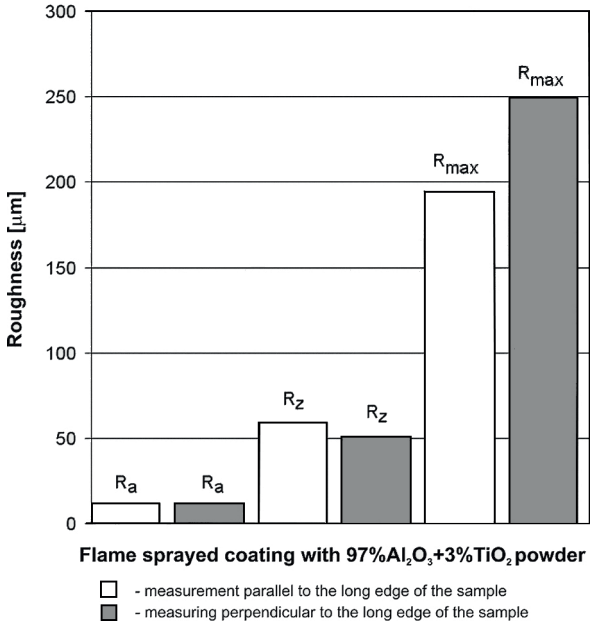

Fig. 9. Roughness parameters R_a, R_z, R_{max} of flame sprayed coating with 97%Al_2O_3+3%TiO_2 powder

Testing of mineral-mineral type abrasion wear resistance of flame sprayed coating with selected powder was carried out on 5×25×75 mm samples in accordance with ASTM G65 standard. The study determined mass consumption of the samples after 100, 125, 250, 500 and 1500 revolutions of disc blade clamping abrasion. Testing results are presented in Table 4.

TABLE 4

Results of tests of abrasion of coatings sprayed with 97%Al_2O_3+3%TiO_2 powder

No. of sample	Revolutions [n]	No. of test	Weight loss [g]	Mean weight loss [g]	Volume loss [mm^3]
1	1500	1	0.8320	0.8314	207.85
		2	0.8310		
		3	0.8311		
2	500	1	0.4397	0.4387	109.66
		2	0.4390		
		3	0.4375		
3	250	1	0.1914	0.1840	92.00
		2	0.1906		
		3	0.1701		
4	125	1	0.2073	0.2074	51.85
		2	0.2073		
		3	0.2073		
5	100	1	0.1285	0.1283	32.07
		2	0.1284		
		3	0.1279		

The erosion resistance test was conducted in accordance with ASTM G76-95 standard on 5×25×75 mm samples. Alumina (Al_2O_3) powder with particles in sizes of 45÷70 μm was used as and erosive material. The test was conducted with a mean particle speed of 70±2 m/s, an erodent flow rate of ca. 2g/min, a sample to nozzle distance of 10 mm, and incident angle of the abrasive stream of 90°, 60°, 30° and 15°. Time of test was 10 minutes. Results of the test are shown in Table 5 and on Figure 10.

TABLE 5

Value of weight loss in erosion tests of coating sprayed with 97%Al_2O_3+3%TiO_2 powder

Erodent incident angle [°]	Weight of the sample before the test [g]	Weight of the sample after the test [g]	Weight loss [g]
90°	73.8752	73.8703	0.0049
45°	73.8703	73.8485	0.0218
30°	73.8485	73.8206	0.0279
15°	73.8206	73.8027	0.0179

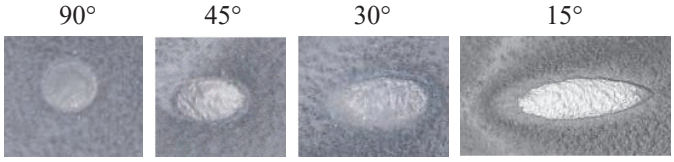

Fig. 10. View of surfaces coating sprayed with 97%Al_2O_3+3%TiO_2 powder after the erosion tests, 4× mag

Coating adhesion testing, Rh (pull-off strength) was determined in a static peel tensile test in accordance with EN 582:1996 standard on cylindrical samples with Ø40 mm diameter. The front surface of cylindrical samples coated with adhesive was adhered to a counter sample Henkel Locit Hysol 3478 A&B Superior Metal glue with a tensile strength of 17 MPa. Samples with a fastening device were placed in a testing apparatus and subjected to static stretching until a break point was reached, Figure 11. Results of tensile test allowed for the determination of the strength of detachment of the coating from the substrate and to calculate the coefficient of adhesion Table 6.

TABLE 6

Results of adhesion test for coatings sprayed with 97%Al_2O_3+3%TiO_2 powder

No. of sample	Dimensions of the sample		Maximum breaking force [N]	Coefficient of Adhesion [N/mm^2]	
	Diameter [mm]	Cross-section area [mm^2]		R_h	$R_{hśr}$
1	39.4	1218.6	7614.0	6.0	6.5
2	39.0	1193.9	6418.0	5.4	
3	39.8	1243.5	10095.0	8.1	

Fig. 11. Exemplary rupture of sample with coating sprayed with 97%Al_2O_3+3%TiO_2 powder

Testing the thermal shock resistance was conducted in accordance with ISO 14923:2003 on 5×25×75 mm samples. Because of the lack of detailed instructions referring to performing such tests this type of testing was established to occur in three stages:

- first stage – heating to a temperature of 1050 °C and slow cooling in a furnace at a rate of 40°/h,
- second stage – heating to the temperature of 1050 °C and cooling the samples in a stream of compressed air at a rate of 25 °/s, this cycle was repeated ten times,
- third stage – heating to a temperature of 1050 °C and rapidly cooling the samples in water at a rate of 100 °/s. The result of the tests indicated a number of cycles after which the coating surface showed discontinuities and delaminations, Figure 12.

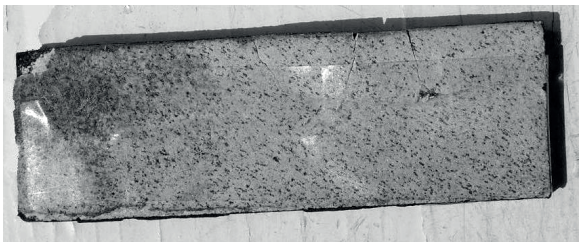

Fig. 12. View of the sample after third stage of thermal shock resistance test

3. Discussion

After conducting the flame spraying process, visual testing allowed for the possibility to determine colour and surface quality of a test plate after flame spraying with 97%Al_2O_3+3%TiO_2 powder. After spraying the sample was characterized with a blue-grey colour, matte finish characterised by a slight waviness. Metallographic examination of the specimens' cross-sectional surface revealed that the surface of the steel developed surface lines which occurred after the successive application of the two coatings: primer coating (B) and outer coating (A), Figure 3 a). Directly above the surface of the base material (C) the primer coating (B) with 30 μm to 110 μm thickness was observed, consisting of bright areas formed of Ni-Al-Mo alloy and dark oxide inclusions, Figure 3 c). In the primer coated border areas there exists a banded structure in the base material, this characteristic is indicative of the strengthening of the steel surface which occurred during shot-blasting of the steel substrate. On the primer coating, an outer coating molding with a thickness ranging from 450 μm to 510 μm was formed during spraying. This coating was characterized with a high amount of voids in varying sizes and a corrugated outer surface, Figure 3 d). Hardness measurements were performed on metallographic specimens in micro-areas of the outer coating (A), the primer coating (B) and the steel base (C), Figure 4. External specific coating sprayed with 97%Al_2O_3+3%TiO_2 powder was characterized with hardness from 670 HV5 to 910 HV5. In the primer coating, the tested micro-areas demonstrated a lower hardness from 350 HV01 to 470 HV01. The base material, hardness in the area bordering the primer coating amounted to ca. 226 HV05, what confirms the occurrence of narrow SWC or surface strengthening of steel after grit blasting. In the distance of ca. 500 μm from the surface, hardness of steel was ca. 110 HV05 that is characteristic for a ferrite structure with small amount of cementite and perlite. XRD studies allowed for identifying phases in the structure of the coating, Figure 5. After spraying the material on an aluminium-matrix the structure of the Al_2O_3, $NiAl_{10}O_{16}$ and $NiAl_{32}O_{49}$ phases have been detected as well as trace amounts of Fe α, Figure 5. Tests did not show the occurrence of titanium, which was added to the spraying powder prior to application(TiO_2=3%). The XRD testing conducted makes it possible to find titanium only if it occurs in amounts over 4% of the total composition. In the diffractogram obtained for the tests the pattern observed showed ten diffraction lines from the Al_2O_3 phase, including those with maximum intensity from planes (113), (116), (124), (030) and (1.0.10). There were also found four diffraction lines coming from planes (121), (212), (400) and (123) $NiAl_{10}O_{16}$ phase and planes (201), (321), (332), (122) NiAl32O49 oxide phase. Also observed were diffraction lines at (100) and (211) occurring with small intensity coming from Fe α. Detailed examination of the internal structure of the coating and the determination of chemical composition in the micro-areas has been conducted using SEM. The outer coating, sprayed with 97%Al_2O_3+3%TiO_2 powder, was not observed to be homogeneous, Figure 6 a). Voids ranging from 10 to 100μm were observed. A small number of voids was also observed in the area bordering the primer coating, Figure 6 b). The width of this area was ca. 40 μm. The outer consisted of adhered particles, Figure 6 c). On the basis of point microanalysis, it has been stated that the particles which occur there are composed of aluminium, titanium, oxygen of wt% concentration of 56.41%, 5.09% and 38.49%, respectively, Figure 8. Surface roughness testing of the ceramic coating in two perpendicular directions including the determination of R_a, R_z and R_{max} values have shown that the coating is characterized with a high surface roughness, Figure 9. Results of abrasion wear resistance tests, have shown that the coating sprayed with the 97%Al_2O_3+3%TiO_2 powder featured high abrasion wear resistance in the researched range of revolutions ranging from 100 rpm to 1500 rpm, Table 5. Based on the erosion wear resistance tests it was observed that sprayed coating features a high abrasion wear resistance (determined through loss of weight). In the case of erosion testing under 45°, 30° and 15° incident angle, the weight loss amounted to 0.0218g, 0.0279g and 0.0179g, respectively. Adherence to the base of the performed coating defined on the basis of the static tensile test till tearing the coating off the base has shown that coating adherence is high and equals to 6.5 MPa, Table 7. Diverse breaking strength force values and coating adhesion values have confirmed the occurrence of non-homogenous cracks of sample surfaces after the tensile test. Resistance to thermal shock has been evaluated with cyclic heating to 1050 °C and cooling at a rate of 40 °C/h (with furnace), 25 °C/s (air stream cooling), 100 °C/s (water cooling). Resistance to thermal shock was demonstrated. After heating the samples up to the temperature of 1050 °C and cooling with a furnace in the first cycle of the test, compressed air cooling in the next nine cycles and cooling in water after the last cycle revealed no failures such as delamination, however, some cracking with tearing absent was observed, Figure 12.

4. Conclusions

Based on the tests conducted and analysing the results obtained, flame spraying with 97%Al_2O_3+3%TiO_2 powder selected technical parameter range allows for the preparation of high-quality ceramic coatings with ca. 500 μm thickness on the selected steel substrate. The flame sprayed coating has a confirmed composition consisting mainly of aluminium oxide and small amounts of $NiAl_{10}O_{16}$ and $NiAl_{32}O_{49}$ phases. Bonding the Ni-Al-Mo primer powder to the steel base and externally coating with the 97%Al_2O_3+3%TiO_2 demonstrates the characteristics of a mechanically bound coating. The coating is characterized by high adhesion to the substrate with an adhesive force of 6.5 MPa. The average hardness of the outer coating is ca. 780 HV. The resulting coatings are characterized with high erosion, abrasive wear and cyclic thermal shock resistance.

Acknowledgements

This work was supported by the Faculty of Mechanical Engineering of the Silesian University of Technology in 2015 as the subsidy for statutory activity.

REFERENCES

[1] S.J. Matthews, B.J. James, M.M. Hyland, Mater. Charact. **58**, (1) 59-64 (2007).

[2] D. Janicki, Solid State Phenom. **199**, 587-592 (2013).

[3] A. Arcondéguy, G. Gasgnier, G. Montavon, B. Pateyron, A. Denoirjean, A. Grimaud, C. Huguet, Surf. Coat. Tech. **202**, (18), 4444-4448 (2008).

[4] J.F. Li, L. Li, F.H. Stott, Thin Solid Films **453-454**, 67-71 (2004).

[5] E. Torres, D. Ugues, Z. Brytan, M. Perucca, J. Phys. D Appl. Phys. **42**, (10), 105306 (2009).

[6] A. Lisiecki, Metals, **5**, (1), 54-59 (2015).

[7] D. Golański, G. Dymny, M. Kujawińska, T. Chmielewski, Solid State Phenomena, **240**, 174-182 (2015).

[8] A. Czuprynski, J. Gorka, M. Adamiak, Metalurgija **55**, (2), 173-176 (2016).

[9] C. Li, G. Yang, Z. Wang, Mater Lett. **57**, (13-14), 2130-2134 (2003).

[10] A. Arcondéguy, G. Gasgnier, G. Montavon, B. Pateyron, A. Denoirjean, A. Grimaud, C. Huguet, Surf Coat Tech., **202**, (18) 4444-4448 (2008).

[11] J. Gorka, A. Czuprynski, Appl. Mech. Mater. **809-810**, 501-506 (2015).

[12] Y. Lian, L. Yu, Q. Xue, Wear **181-183**, (1), 436-441 (1995).

[13] Yu. Borisov, A. L. Borisova, Ceram. Int. **9**, (4), 138-141 (1983).

[14] C.J. Li, G.J. Yang, Z. Wang, Mater. Lett. **57**, (13-14), 2130-2134 (2003).

[15] M. Bonek, G. Matula, L.A. Dobrzanski, Adv. Mat. Res. **291-294**, 1365-1368 (2011)

[16] F. Vargas, H. Ageorges, P. Fournier, P. Fauchais, M.E. López, Surf. Coat. Tech. **205**, (4), 1132-1136 (2010).

[17] A. Góral, W. Żórawski, L. Lityńska-Dobrzyńska, Mater. Charact. **96**, 234-240 (2014).

[18] Z. Glogovic, V. Alar, Z. Kozuh, I. Stojanovic, S. Kralj, Materialwiss. Werkst. **42**, (3) 224-228 (2011).